DISCLAIMER

This report was prepared as an account of work sponsored by an agency of the United States Government. Neither the United States Government nor any agency thereof, nor any of their employees, makes any warranty, express or implied, or assumes any legal liability or responsibility for the accuracy, completeness, or usefulness of any information, apparatus, product, or process disclosed, or represents that its use would not infringe privately owned rights. Reference herein to any specific commercial product, process, or service by trade name, trademark, manufacturer, or otherwise does not necessarily constitute or imply its endorsement, recommendation, or favoring by the United States Government or any agency thereof. The views and opinions of authors expressed herein do not necessarily state or reflect those of the United States Government or any agency thereof. Reference herein to any social initiative (including but not limited to Diversity, Equity, and Inclusion (DEI); Community Benefits Plans (CBP); Justice 40; etc.) is made by the Author independent of any current requirement by the United States Government and does not constitute or imply endorsement, recommendation, or support by the United States Government or any agency thereof.

Final Report

Particle dynamics in the spatial afterglow of flowing dusty plasmas

Department of Energy - DE-SC0022242

Principal Investigator: Professor Uwe R. Kortshagen

Department of Mechanical Engineering

University of Minnesota

111 Church Street SE

Minneapolis, MN 55455

phone: (612) 625 4028, fax: (612) 626 1854, kortshagen@umn.edu

Co-Principal Investigator: Professor Christopher J. Hogan

Technical Contact:

Dr. Nirmol Podder, podder@science.doe.gov

November 30, 2025

I. Overview:

Dusty plasmas occur throughout the universe from interstellar nebulae, to planetary rings, to dust tails of comets, to plasmas in laboratories and semiconductor manufacturing. The vast majority of laboratory dusty plasma research has focused on situations during the active plasma phase, meaning when an electric field is applied to sustain the plasma in a steady state.

However, every laboratory or industrial plasma will eventually be turned off, exposing dust to the rapidly decaying plasma "afterglow". Equally, in space plasmas dust may experience conditions of rapid plasma decay. Compared to the rich literature on dust in steady-state plasmas, understanding dust dynamics in afterglow plasmas is a little-studied, unresolved scientific problem of tremendous importance for technological plasma applications. For instance, the formation of particles as small as a few nanometers may cause fatal defects in semiconductor processing.

One aspect studied in this project, which is largely ignored in dusty plasma research, is the impact of dust grains on the properties of the dusty plasma. However, these material properties significantly impact the kinetics of particle charging and discharging, as well as the dynamics of particle aggregation and growth in the afterglow. Hence, this project studied the largely unexplored material dependencies governing particle decharging and particle agglomeration in the afterglow.

The overarching hypothesis of this project was that the particle dynamics in the afterglow of dusty plasmas are determined by the interplay of the transient plasma properties and the material properties of dust particles. By combining experiments and modeling in an approach fundamentally different from prior research, this project investigated correlations between material properties and basic dust charging and decharging mechanisms.

Extensive plasma diagnostics were utilized to determine essential plasma properties. In doing so, we discovered that double Langmuir probes get significantly affected by the presence of particles, and we developed a model to address the impact of the dust particles on the Langmuir probe characteristics.

II. Highlighted accomplishments:

1. Material Dependence of Particle Agglomeration in the Afterglow of Pulsed Plasmas

Initially, we studied the agglomeration of submicron-sized particles in the afterglow of a pulsed capacitively coupled plasma. Experiments were conducted in the parallel-plate capacitively coupled plasma (CCP) reactor shown in Figure 1a. This reactor is based upon the Gaseous Electronics Conference RF reference cell. In it, a plasma is maintained between two planar aluminum electrodes, each 20 cm in diameter and separated by a 2.5 cm gap. The upper plate is powered by a 13.56 MHz radiofrequency (RF) sinusoidal waveform from a function generator (BK Precision model 4063); the waveform power is amplified with an ENI RF power amplifier model 3200L, and a matching box (Vectronics model HFT 1500) is connected to the amplifier to minimize the reflected power during operation. The bottom electrode is connected to ground potential.

The reactor has three side inlet and outlet ports for flow, as well as a flow line connected underneath the bottom electrode. Figure 1b depicts all gas inputs and outputs. The CCP reactor was operated with Ar gas at pressures ranging from 0.1 Torr – 2 Torr (13.3-266 Pa). To generate a dusty plasma, after sealing the inlet line and exhaust line, Ar gas was pulsed (at 200 sccm) through the upper side injection tube over a

particle bed (0.635 cm in diameter and 12 cm in length); the bed was loaded with 1 mg of particles of the desired material properties (commercial micropowders). Particle mass loadings above 1 mg were also used in selected experiments (but within an order of magnitude of 1 mg). Six different particle materials were utilized, with dielectric constants ranging from 5.8-1200 in the 10-20 MHz range, Table 1. Particle trapping and agglomeration were observed at the upper electrode of the CCP reactor. Figure 1c shows the directions of the relevant forces acting on the particles at this location.

Table 1. The properties of the test particles used in trapping experiments.

Material	Chemical formula	Dielectric constant	Density (g cm^{-3})	Electron affinity (eV)
Borosilicate	SiO_2	5.8	2.50	1.30
Iron (III) oxide	Fe_2O_3	6.8	5.24	4.82
Zinc Oxide	ZnO	8.5	5.60	4.30
Zirconium Oxide	ZrO_2	12.5	5.89	3.43
Titanium Dioxide (rutile)	TiO_2	110	4.23	4.69
Barium Titanate	$BaTiO_3$	1200	5.85	3.90

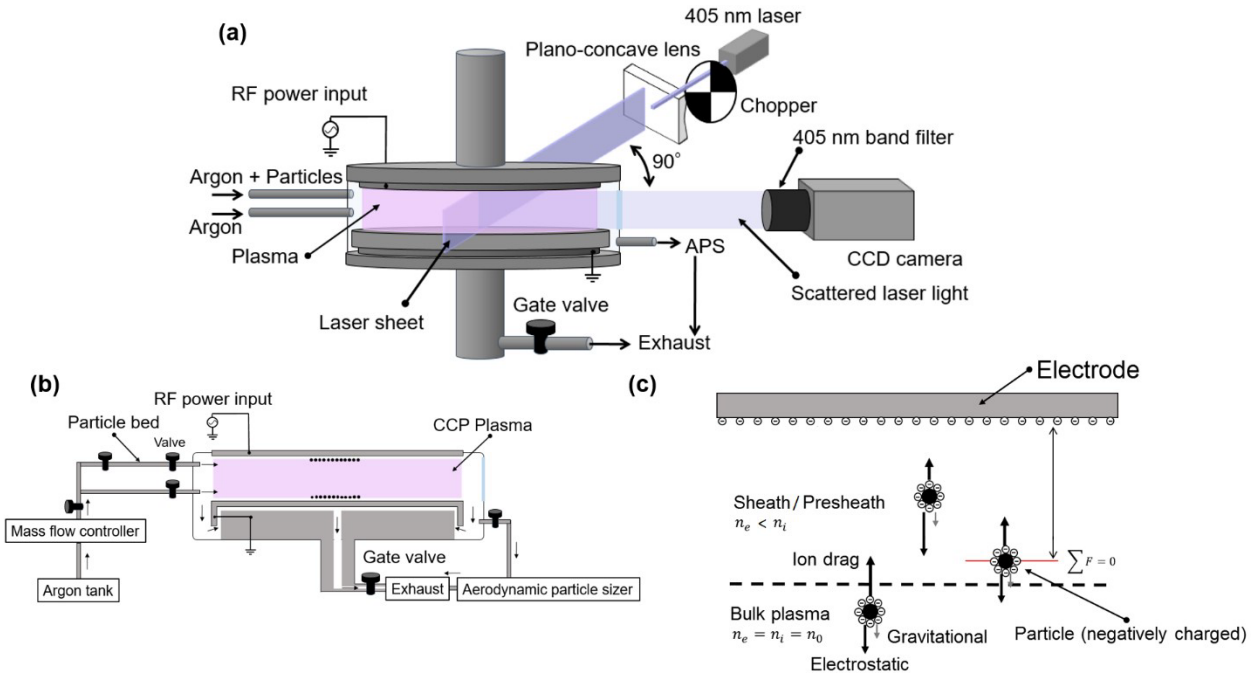

Figure 1. (a) A schematic diagram of the CCP plasma reactor and the laser light scattering (LLS) system used to monitor particle trapping. A 405 nm diode laser is converted into a sheet of light by the Plano-concave lens. Particles scatter light as they cross the laser sheet, and the CCD camera captures the scattered light. Light emitted by the plasma is filtered by a bandpass filter. (b) A cross-sectional view of the reactor showing valve locations. (c) A depiction of the particle trapping location near the top electrode. A balance between the electrostatic force (in the direction away from the electrode for negatively charged particles), the ion drag force (towards the electrode), and the gravitational force (away from the top electrode) determines the particle trapping location.

Dispersed submicrometer particles were exposed to drastically varying ion and electron densities during both ignition and extinction of a non-thermal plasma. The behavior of particles during such events has not been thoroughly studied. We performed laser scattering experiments to examine the behavior of initially submicrometer particles (440 nm–565 nm in radius) as the plasma is pulsed at frequencies ranging from 2 Hz to 0.2 Hz. Pulsing enabled examination of particle behavior in a transient afterglow and during plasma reignition.

During plasma operation, particles are negatively charged and trapped near the sheath boundary at the upper electrode of the horizontally aligned reactor. When the plasma was extinguished, we found size-dependent particle behavior. Initially, particles migrated towards the upper electrode. A small remaining negative bias was measured on the top electrode, suggesting that particles in the afterglow may actually acquire positive charge, as had recently been reported by Goree and coworkers (Physics of Plasmas 28 (10), 103702, 2021). Differential particle speeds during migration to the electrode and to the sheath boundary upon plasma reignition facilitate particle agglomeration during pulsing. In contrast to the initial behavior, the agglomerates first formed by repetitive plasma pulsing migrated downward gravitationally when the plasma in extinguished. By progressively decreasing the pulsing frequency, agglomerates grew further, with agglomerate sizes approaching the millimeter scale for SiO_2 submicrometer particles at pulsing frequencies below 1 Hz, Figure 2. Such millimeter-scale agglomerates were highly non-spherical. We observed that during plasma operation, they remained trapped at locations closer to the upper electrode than smaller agglomerates. Unlike smaller agglomerates, they migrated towards the upper electrode when the plasma was extinguished. This suggests the discharging time for both the original submicrometer particles and for millimeter-sized agglomerates is 10^2-10^3 ms, similar in magnitude to the pulse period.

We found that the pulsing frequencies that lead to agglomerated silica particles do not lead to equally large agglomerates with barium titanate particles, Figure 3, suggesting that discharging rates are material dependent. These observations suggest that pulsed plasma systems can control the extent of agglomeration in particulate systems, creating agglomerates multiple orders of magnitude larger than the base primary particles.

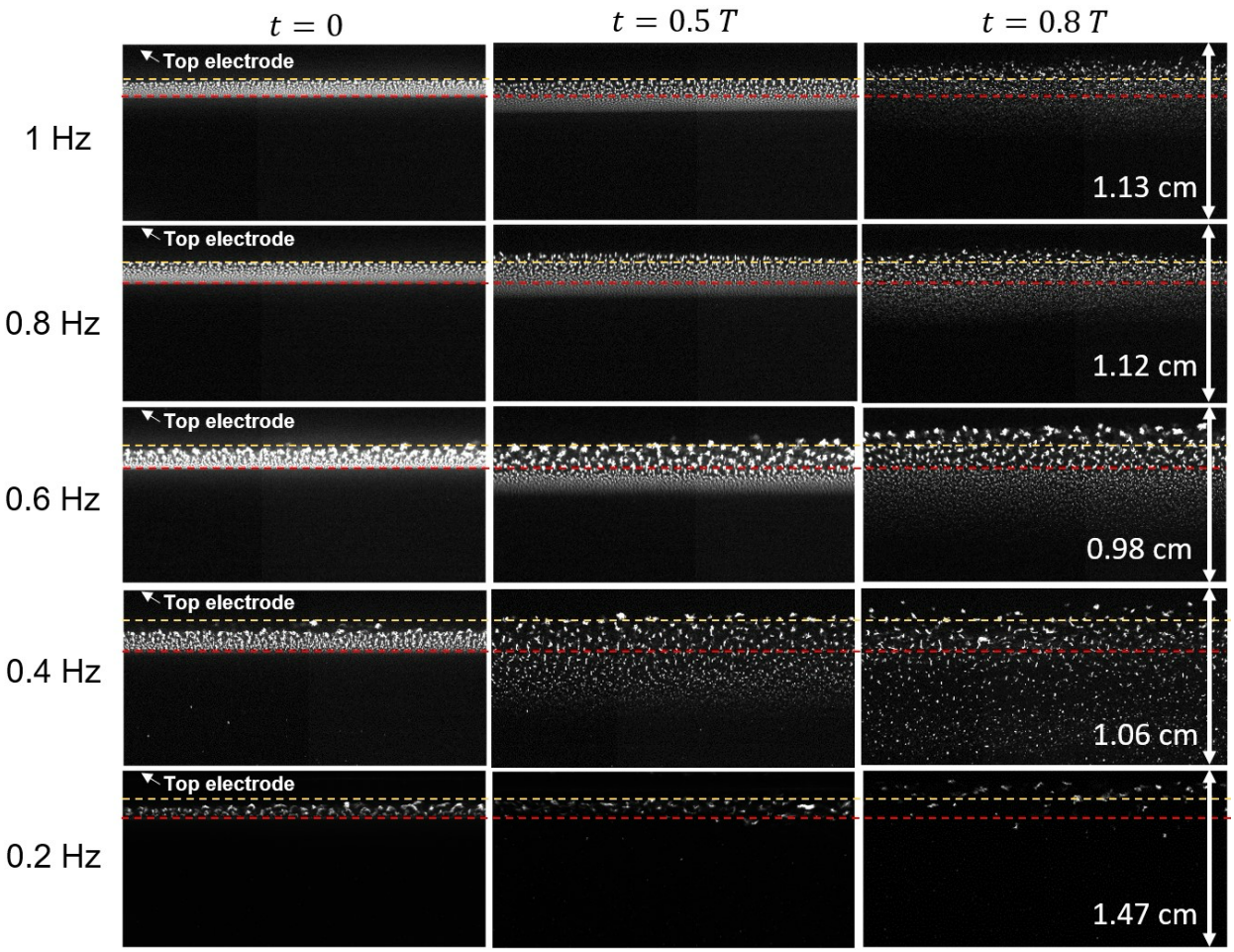

Figure 2. Snapshots of 90° scattered laser light captured with a CCD camera for SiO_2 particles for variable times following plasma extinction and until reigniting the plasma up for frequencies from 1.0 Hz to 0.2 Hz. Horizontal dashed lines bound the trapping region for particles when the plasma is operated (at 0s) in each video.

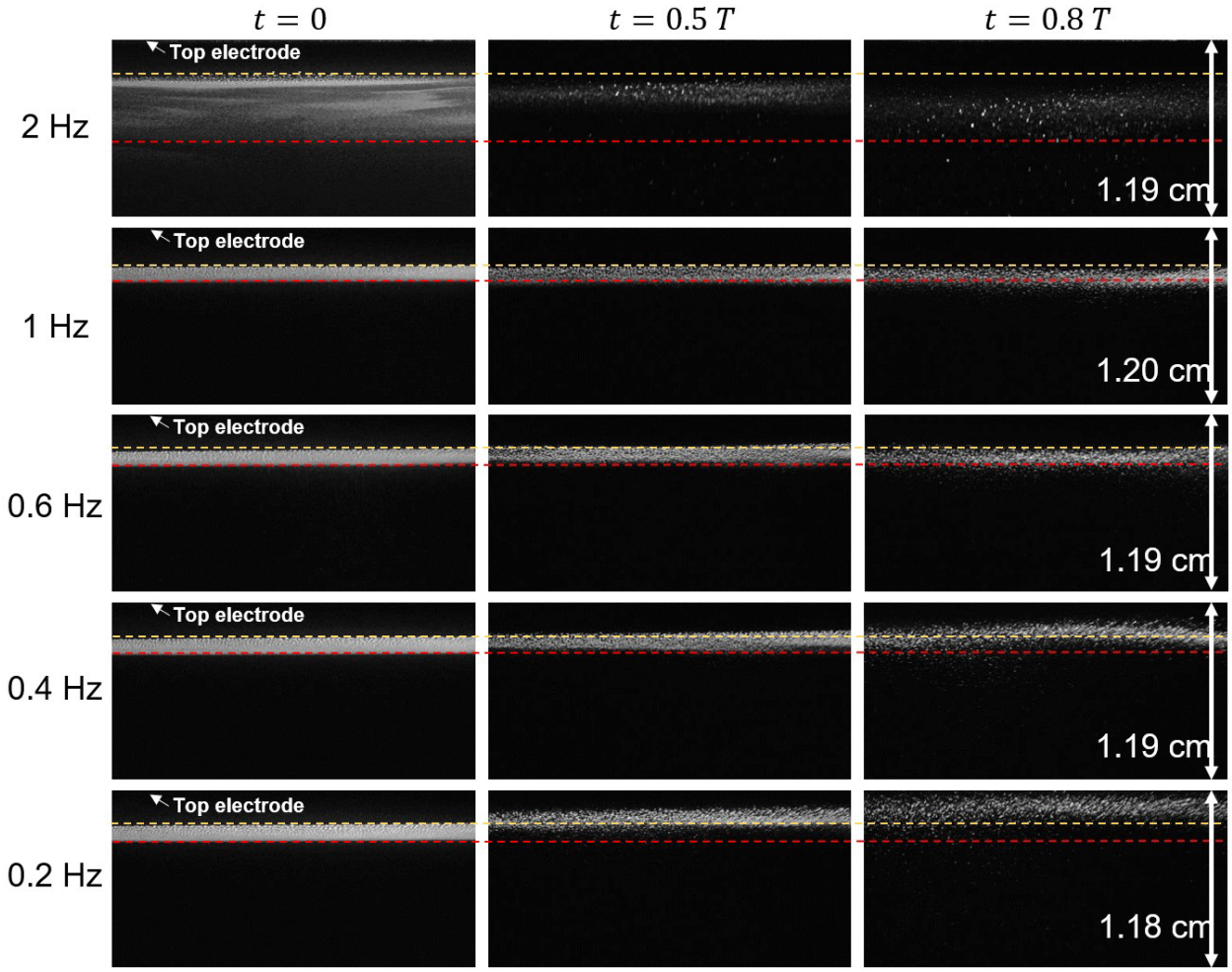

Figure 3. Snapshots of 90° scattered laser light captured with a CCD camera for $BaTiO_3$ particles for variable times following plasma extinction and until reigniting the plasma up for frequencies from 2 Hz to 0.2 Hz. Horizontal dashed lines bound the trapping region for particles when the plasma is operated (at 0s) in each video.

Pulsing the plasma for an extended period of time led to the formation of unexpectedly large particle agglomerates. In an experiment conducted with SiO_2 particles, the plasma was ignited with a continuous Ar flow into the reactor and an open pump. Once the system reached the steady-state close to the desired pressure, the inlet and outlet flows were stopped. 20 mg of dispersed silicon dioxide SiO_2 particles, with an average diameter of 2 μm, were introduced into the plasma through the nozzle using an Ar gas puff. The working pressure was finalized at 133 Pa (1 Torr) prior to the pulsing of the RF signal in the following experiments. The plasma was ignited with an input power of 20 W.

Particles were found trapped near the top electrode after injection, as expected. Continuous pulses at a 0.5 Hz frequency with a 50% duty cycle were applied to the plasma to produce a transient afterglow. During a single pulse, particles settled down to the bottom electrode due to gravity after the plasma was switched off, then quickly returned to the trapping position after the reignition of plasma. Different images are shown in Figure 4 when the plasma was on for different times of pulsing with trapped particles. As time progressed, it became evident that agglomeration, occured with non-spherical and more than millimeter-sized agglomerates floating between the electrodes. This is a remarkable result, as particles this large have not been reported before as being trapped in the plasma.

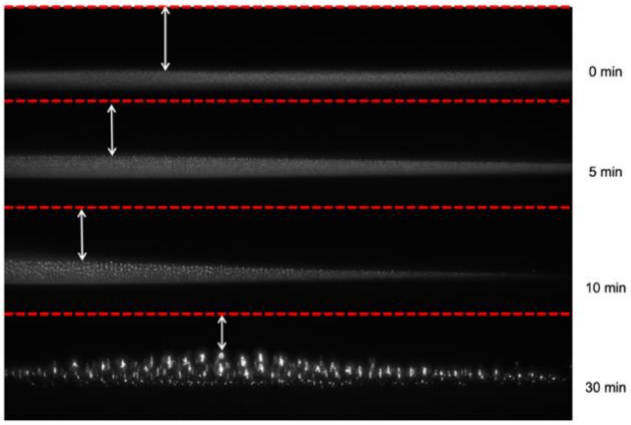

Figure 4: Particle agglomeration with time. Red dashed lines provide the position of the top electrode.

To further understand the particle motion in the afterglow, we analyzed the forces acting on the particle by tracking settling velocities. Figure 5a shows two CCD images, taken at different times, overlaid. One image (t = 0.36 s) corresponds to when the plasma is on, while the other (t = 1.2 s) was taken in the afterglow of the plasma after it was turned off. Particles are visible in the image as a bright horizontal line, created by the laser light scattered from the particles. At t = 0.36 s, particles are trapped roughly 4 mm below the top electrode, located at y = 0 in the picture. However, in the afterglow, particles have dropped down to y = -7 mm. This is because, after switching off the power, the particles were no longer trapped at the plasma sheath of the upper electrode by the ion drag force. Instead, particles began to fall toward the bottom of the reactor, presumably under the influence of gravity. To investigate the forces acting on particles in the afterglow, we tracked particle motion over time using repeatedly acquired CCD images. From the images, we extracted the particle position over time, shown in Figure 5b. The figure shows the mode and mean of the particle position, obtained from the CCD images. At t = 0, the plasma is still on, and particles are trapped at the upper electrode. At t = 0.5 s, the plasma is switched off, and particles begin to fall, as indicated by their positions becoming more negative. At t = 1.5 s, the plasma is switched on again, and particles quickly move back up to the trapping position at the upper electrode's sheath edge. Because of the disparity in trapping positions and intensities for large and small particles, there is a one-millimeter difference in position between the mode and the mean, but the two values generally agree in trend. The results are very reproducible over multiple pulsing cycles, and the position is averaged over 10 cycles to reduce noise. Figures 5c and

5d illustrate the velocity and acceleration profile of a single pulse cycle over a 2-second period by taking the first- and second-time derivative of the position.

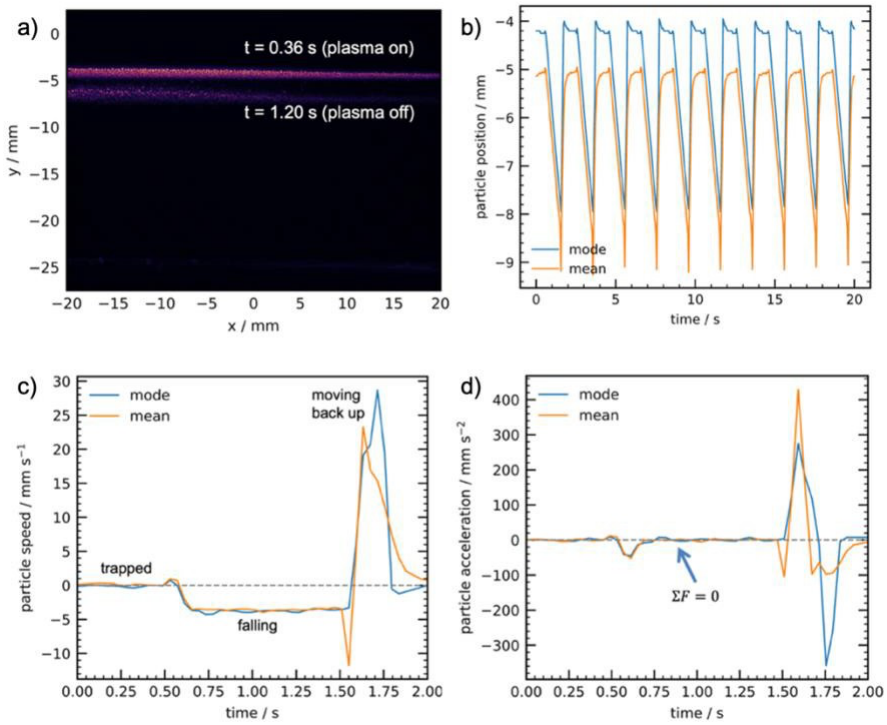

Figure 5: a) Superposition of two images from the CCD camera at t = 0.36 s (plasma on) and t = 1.2 s (plasma off). b) Particle position vs time over 10 2-second pulse cycles. c) Particle velocity vs time. d) Particle acceleration vs time. c) and d) are averaged over 10 cycles. The plasma is switched off at t = 0.5 s and switched on at t = 1.5 s.

2. Precursor-free Particle Growth after Initial Particle Generation

In dusty plasma research, it is commonly accepted that the generation and growth of nanoparticles in plasmas requires the presence of a precursor. Multiple studies of capacitive discharges observed that when the precursor flow is terminated, particles tend to shrink, likely due to ion bombardment or etching by some of the flowing gases.

In this project, we observed an opposite behavior. In a study focusing on carbonaceous particles, submicrometer particles were synthesized in a capacitively coupled C_2H_2/Ar plasma. To monitor particle size distributions, the negatively charged particles were electrostatically accelerated towards a biased substrate in contact with the plasma, enabling periodic particle extraction during growth without interrupting the plasma process for subsequent scanning electron microscope (SEM) analysis.

Interestingly, we observed that after an initial precursor injection period of 1 minute, during which particles grow to a radius of ~ 70 nm, particles continue to grow in the plasma without further precursor injection for the next ~40 minutes, Figure 6a. As growth continued, particles trapped at the grounded bottom electrode became less polydisperse, with geometric standard deviations decreasing from 1.18 to 1.02.

To understand this behavior, we performed laser extinction measurements (LEM) to determine the temporal evolution of the particle density using Rayleigh-Mie scattering theory, Figure 6b. The LEM measurements indicated that after the turn-off of the precursor flow after 1 min, the particle density declined from ~$6 \times 10^{14}\ m^{-3}$ to ~$3 \times 10^{11} m^{-3}$ after 46 minutes, while the particle radius increased from ~70 nm to ~480 nm over the same time.

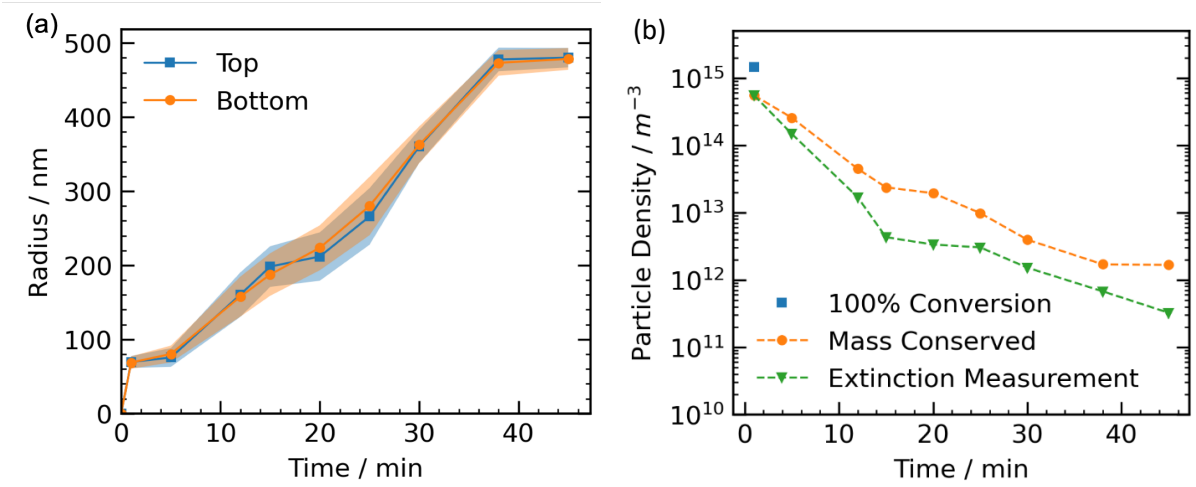

Figure 6: (a) Particle radius as a function of time, determined from SEM measurements at selected times. The shaded area represents the standard deviation from a log-normal fit. (b) Particle density evolution over time, derived from laser extinction measurements (LEM). The green line with triangular markers represents the measured particle density from LEM, while the orange line with circular markers shows the predicted density assuming total mass conservation of particles for the particle diameters in (a). The blue dot indicates the theoretical density if all precursor gases were fully converted into particles.

We rationalized these results by proposing that material may be released from smaller particles and redeposited onto larger particles. This is analogous to Ostwald ripening, though it may be distinct in the underlying mechanism; Ostwald ripening is typically driven by the elevated surface concentrations or vapor pressures of smaller particles, leading to their evaporation in systems with lower precursor concentrations than the particle surface concentration. Meanwhile, larger particles, with surface concentrations below the background concentration, are stable and grow.

We hypothesized that in the nonthermal plasma environment, the preferential heating of smaller particles may lead to their dissociation, and the subsequent growth of larger, highly monodisperse particles, which experience diminished heating. These results suggest that selective, size-dependent heating may play an important role in particle growth dynamics in non-thermal plasmas.

Further analysis of these data is still in progress as the Ph.D. student on this project completes her thesis work.

3. Langmuir Probes in Dusty Plasmas

Due to the need to determine plasma properties in our dusty plasma environment, we utilized double probes for measurements of the electron temperature and the positive ion density. However, when using the double probe in a dusty plasma operating in argon:silane, we made a very surprising observation of seemingly unreasonably large electron temperatures when silicon particles formed in the plasma, as shown in Figure 7.

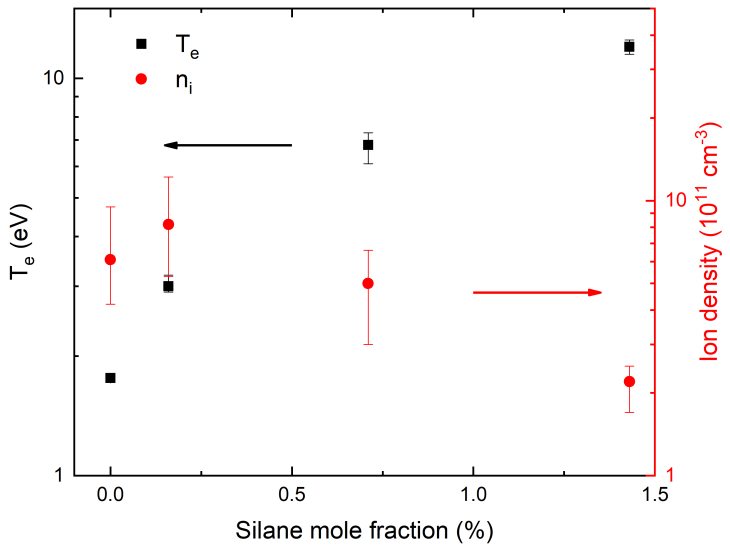

Figure 7: Electron temperature (■) and ion density (●) as a function of silane mole fraction on a logarithmic scale. The error bars indicate maximum and minimum values of three consecutive measurements.

To test whether electron loss to the particles could be responsible for these large electron temperatures, we developed a zero-dimensional global model to investigate the effect of the presence of nanoparticles on the plasma properties. Using this model, we showed that increasing particle concentration leads to an increasing electronegativity of the plasma, causing an increase in the reduced electric field. However, this causes only a moderate increase in mean electron energy, in contrast to the much larger increase measured by the double probe.

We then proposed that these large electron temperatures are based on the fact that a double probe measures an "apparent" electron temperature, which is defined by the negative inverse slope of the logarithm of the electron energy probability function (EEDF) at an energy corresponding to the probe's floating potential. As the silane mole fraction increases, the plasma becomes more electronegative, and the probe's floating potential shifts closer to the plasma potential. Combined with the strong non-Maxwellian EEDF, this leads to the large apparent electron temperatures obtained by the probe, Figure 8. This model was found to be indeed consistent with the temperatures indicated by the double probe. Thus, the apparent electron temperatures measured with the double probe **do not follow** the trends of the mean electron energy of the electron energy distribution function. The "temperature" measured by the double probe should thus not be mistaken for accurately indicating the electron temperature in a dusty plasma. This study was published in *Plasma Sources Science and Technology.*

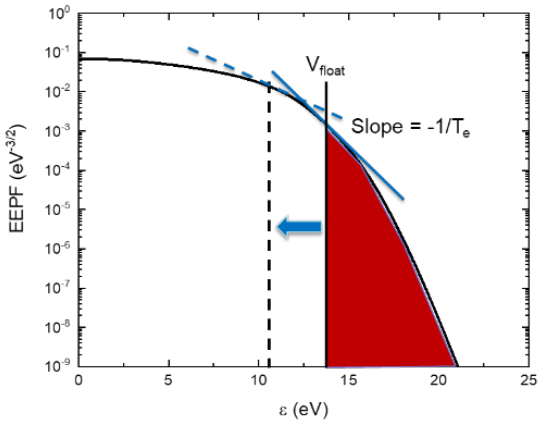

Figure 8: Illustration of the elevated "apparent electron temperature" T_e measurements by the double probe in an electronegative plasma. T_e is proportional to the inverse slope of the electron energy probability function (EEPF) at the electron energy equal to the particle floating potential. As the plasma becomes more electronegative due to particle formation, the floating potential shifts to lower electron energies, as indicated by the blue arrow, due to the reduced electron flux. For the same EEPF, this causes a larger apparent electron temperature to be measured by the double probe.

III. Products

Journal publications:

[1] Tamadate T and Hogan C J 2022 Silicon nanocluster anion-argon cation recombination via hybrid continuum-molecular dynamics calculations *JOURNAL OF AEROSOL SCIENCE* 163

[2] Xiong Z, Held J and Kortshagen U 2023 Reliability of double probe measurements in nanodusty plasmas *Plasma Sources Sci. Technol.* 32 035001

[3] Beckers J, Berndt J, Block D, Bonitz M, Bruggeman P J, Couëdel L, Delzanno G L, Feng Y, Gopalakrishnan R, Greiner F, Hartmann P, Horányi M, Kersten H, Knapek C A, Konopka U, Kortshagen U, Kostadinova E G, Kovačević E, Krasheninnikov S I, Mann I, Mariotti D, Matthews L S, Melzer A, Mikikian M, Nosenko V, Pustylnik M Y, Ratynskaia S, Sankaran R M, Schneider V, Thimsen E J, Thomas E, Thomas H M, Tolias P and Van De Kerkhof M 2023 Physics and applications of dusty plasmas: The Perspectives 2023 *Physics of Plasmas* 30 120601

[4] Chen X, Yang H and Hogan C 2024 A constant number Monte Carlo approach to examine Non-Isothermal nucleation and growth in a limited vapor system *CHEMICAL ENGINEERING JOURNAL* 483

Conference Presentations:

[1] Y. Zhao, J. Held, C. Hogan, U. Kortshagen, Particle growth in a dusty plasma without precursor flowing, 2024 Dusty Plasma Workshop, Minneapolis, MN.

[2] Y. Zhao, J. Held, C. Hogan, U. Kortshagen, Precursor-free particle growth in a dusty plasma, 2024 ICOPS, Beijing, China.

[3] J. Held, W. Villafana, I. Kaganovich, U. Kortshagen, New model for the ion collection by cylindrical probes over a wide range of collisionality, APS Gaseous Electronics Conference, 2023, id.ET2.001, Ann-Arbor, Michigan.

There are still several more manuscripts in preparation or under review.

IV. Training Opportunities

During the current reporting period, one postdoctoral researcher and graduate students participated in the research:

Post-doctoral researchers/research scientists:

1. Dr. Julian Held

Graduate student researchers:

1. Ms. Yue Zhao

The graduate Student and post-doc were exposed to an interdisciplinary training environment, which involves research in experimental plasma physics, materials chemistry, and computational plasma simulation.

Dr. Julian Held participated in the research with a fraction of his effort. After one and a half years at the University of Minnesota, Dr. Held started a position as a tenure-track assistant professor at the Eindhoven University of Technology (TUE).

Ms. Yue Zhao started on the project as a new Ph.D. student in Chemical Engineering at the University of Minnesota. She conducted the majority of the experimental studies on this project. Ms. Zhao is currently finishing up the remaining work for her Ph.D. thesis.

V. Technology Transfer

None